Seismogenic Thickness of the Andean Crust

Martin Andrés Riedel[1], Andrés Tassara[2], Catalina Cabello[2], Denisse Leal[2], and Mauro Castillo[2]

[1]Univerdidad de Concepción
[2]Universidad de Concepción

August 31, 2023

Abstract

The thickness of the seismogenic crust (Ts) controls crustal earthquakes. Its upper limit is the seismicity onset depth (SOD) while its base corresponds to the seismicity cutoff depth (SCD) that correlates with the brittle-ductile transition. Thus, it influences the magnitude and location of crustal earthquakes and knowledge of its geometry may aid in seismic hazard assessment. Here we present the first Ts map of the Andean margin. We follow the standard methodology using the statistical depth distribution of events on a grid of equally size square cells. However, we find it has flaws and develop a new approach, based on circular cells of variable radius that changes according to earthquake density. Our results indicate that Ts is heterogenous, showing three controls: thermal structure, subduction geometry and crustal thickness.

Seismogenic Thickness of the Andean Crust

M. Riedel[1,2], A. Tassara[1,2], C. Cabello[1,2], D. Leal[1,2] and M. Castillo[1]

[1] Departamento Ciencias de la Tierra, Universidad de Concepción, Chile.

[2] Millenium Nucleus The Seismic Cycle along Subduction Zones (CYCLO).

Corresponding author: Martin Riedel (mriedel@udec.cl)

Key Points:

- We propose a new method to calculate seismogenic thickness, particularly for areas with heterogenous hypocenter distribution
- We calculate the seismogenic thickness for the Andean crust.
- We discuss seismogenic thickness implications for seismic hazard assessment.

Abstract

The thickness of the seismogenic crust (Ts) controls crustal earthquakes. Its upper limit is the seismicity onset depth (SOD) while its base corresponds to the seismicity cutoff depth (SCD) that correlates with the brittle-ductile transition. Thus, it influences the magnitude and location of crustal earthquakes and knowledge of its geometry may aid in seismic hazard assessment. Here we present the first Ts map of the Andean margin. We follow the standard methodology using the statistical depth distribution of events on a grid of equally size square cells. However, we find it has flaws and develop a new approach, based on circular cells of variable radius that changes according to earthquake density. Our results indicate that Ts is heterogenous, showing three controls: thermal structure, subduction geometry and crustal thickness.

Plain Language Summary

Most crustal earthquakes occur within a layer of the continental crust known as the seismogenic crust (Ts). Its thickness influences how mechanically strong or weak the crust is and how deep earthquake ruptures may propagate. Therefore, knowledge of Ts's geometry may help constrain future earthquake's location and magnitude, helping to prepare for such events and reduce their impact on society. Here we create the first Ts map in the Andean margin. We do this by calculating the statistical distribution of earthquakes within the crust using two different methods. The first, traditionally used in bibliography, uses a grid of equally sized square cells and calculates the depth distribution of events in each cell. We find that it has flaws and therefore develop the new one. It uses circular cells of variable radius according to earthquake density. We find that Ts thickness in our study area is highly variable and may be controlled by the temperature distribution within the crust, crustal thickness, and the geometry of the interface between the Nazca and South American plates. Ts is particularly thin close to the coastline and to the Andes cordillera. Focalizing crustal earthquake mitigation measures on those regions may help reduce their impact.

1 Introduction

The seismogenic zone is the layer of Earth's crust where most earthquakes occur (Eaton *et al.,* 1970 and Sibson, 1982). Its thickness (Ts) is the depth difference between its lower and upper boundaries or, respectively, the seismicity cutoff depth (SCD) and the seismicity onset depth (SOD, Sibson, 1982 and Wu *et al.,* 2017). The SOD is generally found on or near the surface while the SCD is related to the brittle-ductile transition (BDT), making Ts equivalent to the brittle crustal thickness (Zuza y Cao, 2020 and references therein). Therefore, to a certain extent, Ts controls the magnitude of crustal earthquakes, as it determines the maximum width faults may achieve. Furthermore, a thin brittle crust is inherently weaker (Burov, 2010) and may fracture more easily, concentrating more earthquakes (Zuza y Cao, 2020), so Ts also exerts control on earthquake locations.

Considering these factors, knowledge of the geometry and thickness of the seismogenic crust can help understanding crustal fault behavior. To that end, previous authors have used seismicity catalogues to constrain the depth of the SOD and/or SCD (eg.: Nazareth y Hauksson, 2004, Chiarabba y De Gori, 2016, Wu *et al*., 2017 and Zuza y Cao, 2020). Most of these studies have been carried out in California or Italy, where abundant crustal seismicity and dense seismic networks provide high resolution data.

To date, SOD and SCD have not been estimated in Chile. Here, the Nazca Plate subducts bellow the South American Plate at a rate of 66 mm/yr, with a NE convergence vector, oblique to the trench (Kendrick *et al*., 2003). Due to the angle of subduction and geological history, three important geomorphological units form, oriented approximately north-south. From west to east these are: the Coastal Cordillera, Central Valley and Andes Cordillera. The geometry of the subducted Nazca slab varies greatly from north to south. Particularly, between ~27ºS and 33.5ºS it subducts at a shallow angle, producing a flat slab segment while subduction is normal to the north and south (Cahill and Isacks, 1992; Tassara and Echaurren, 2012). Due to the coupling of both plates along the megathrust fault, abundant interplate seismicity occurs, producing some of the largest earthquakes ever recorded, such as the 1960 Mw 9.5 Valdivia. Therefore, interplate events have been the focus of most seismic studies in Chile. However, there is historical record of crustal seismicity such as the 1958 Ms 6.3 Las Melosas (Naranjo y Welkner, 2004 and Campos *et al.,* 2005), 2001 Mw 6.3 Chusmiza (Campos *et al.,* 2005) and 2010 Mw 6.9 Pichilemu (Farias et al., 2011) earthquakes. This kind of seismicity has been traditionally overlooked until recently when an important crustal fault, the San Ramon Fault (Armijo *et al.,* 2010) was discovered near Santiago, Chile's capital.

Here, we present the first study mapping SOD and SCD in Chile, using seismic data form the Centro Sismológico Nacional (CSN, figure 1) which has the densest seismic network available at a national scale. We filter the catalogue to obtain crustal earthquakes (figure 1) and use a square grid of equally sized cells to map SOD and SCD as done in previous studies. We also develop a new method using circular cells of varying sizes, determined by earthquake density and compare the results. We believe this new approach is ideal for any contexts where seismicity is heterogenous. Our maps show the geometry and heterogeneity of Ts in the Chilean margin and provide information for the interpretation of its primary controls and for seismic hazard assessment.

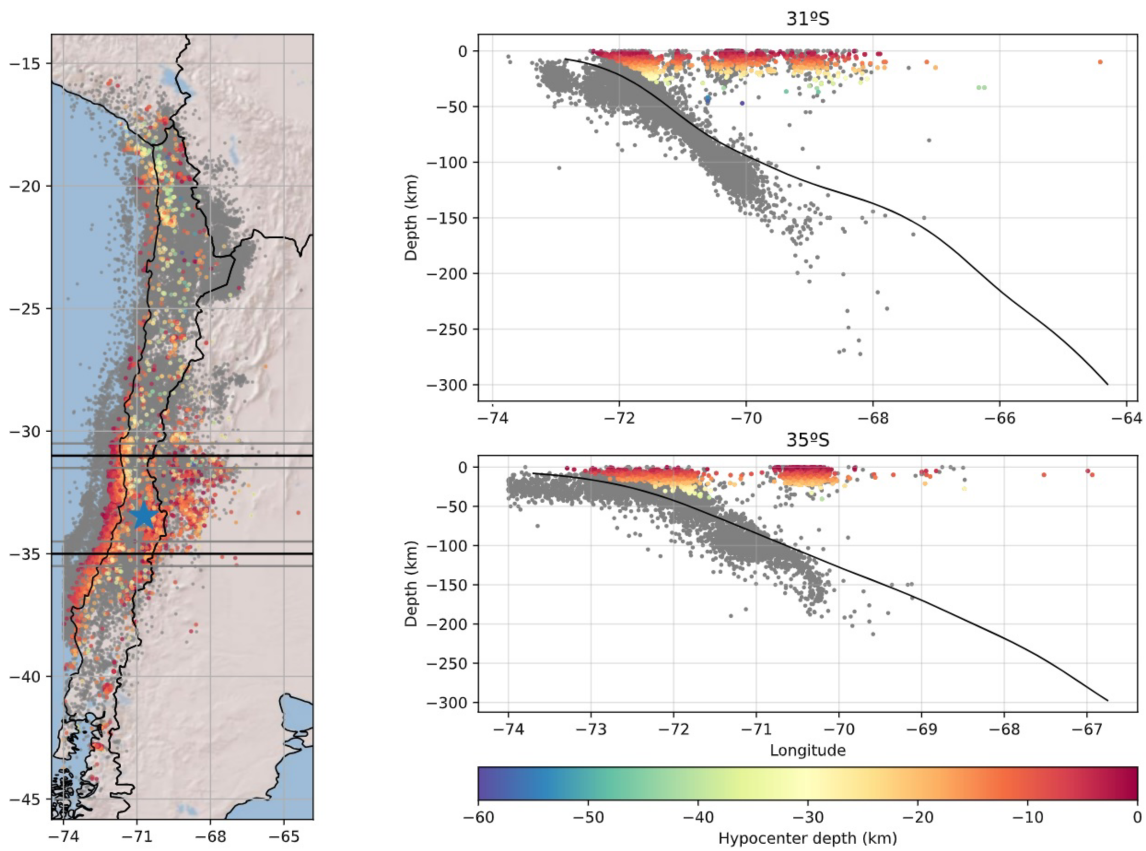

Figure 1: Map (left) of earthquakes in the CSN catalogue (grey) and the filtered crustal earthquakes (color scale). A star indicates the location of Santiago and black lines the location of profiles at 31ºS and 35ºS both of which include seismicity 0.5º north and south of each latitude (grey lines). These profiles (right, 2X vertical exageration) show the depth distribution and slab geometry from Slab2.0 (Hayes, 2018) on different geologic settings: flat slab (31ºS) and normal (35ºS) subduction.

2 Data and Methods

2.1. Seismicity Catalog

For our study we use the CSN seismicity catalogue. In the interest of finding the most complete dataset, we also explored using NEIC and ISC catalogues but these lack the density and precision needed. Local catalogues are also available, with higher resolutions (e.g. Sippl *et al.,* 2018; Sielfeld *et al.,* 2019) but they lack spatial extent. Therefore, the CSN catalogue is the best option. It contains 127336 events between January 1st 2000 and November 2nd 2022 with an average horizontal error of 5.2 km and vertical error of 10.2 km.

To filter the catalogue, we use the 3D geometries of the slab (Hayes *et al.*, 2018) and continental Moho (Tassara y Echaurren, 2012), eliminating all events with hypocenters below these layers. We added a 13 km margin above the slab upper surface following a classification criterion by Sippl *et al.* (2018). We also discard mislocated events (with fixed depth) and those with a vertical or horizontal error larger than 15 km. Ideally a more precise result would be obtained when working with lower errors, however, due to the lesser abundance of crustal seismicity in Chile, deleting to many events would considerably thin out the catalogue. Instead, we choose to keep more events but accompany our data with an average error map to reflect areas of higher or lower confidence in our results.

Finally, due to the heightened capacity of seismic networks to register small crustal earthquakes that are close to stations or the surface, it is necessary to filter events below the catalogue's magnitude of completeness (Mc). We calculate the whole catalogue's Mc using the maximum curvature technique (Mignan y Woessner, 2012) and obtain Mc=2.9.

The above-mentioned filters result in a catalogue with 6654 well located crustal earthquakes (figure 1).

2.2. Determination of SOD, SCD and Ts

Generally, there are two approaches to calculate Ts. As its lower boundary is related to the BDT in the crust, it can be estimated through thermomechanical modeling. However, parameter assumptions (eg. steady-state conditions, rock type, water content, etc.) result in imprecise estimations (Zuza and Cao, 2020). Another method, applied here, is to use the depth distribution of crustal seismicity. However, most studies only calculate SCD and ignore SOD or assume it lays on the surface (eg.: Nazareth y Hauksson, 2004, Chiarabba y De Gori, 2016 and Zuza y Cao, 2020). Furthermore, since SOD and SCD occur over a broad depth range, there is no clear percentile of seismicity to use as proxy for them. For example, percentiles 90, 95 and 99 (hereafter D90, D95 and D99) have all been used. Wu *et al*. (2017) solve this issue by calculating D1, D5 and D10 as proxies for SOD and D90, D95 and D99 for SCD. They then calculate Ts as D99-D1, D95-D5, and D90-D10, thus having thick, intermediate and thin estimates. In this paper we follow the same approach.

The methodology used to calculate each percentile is generally standard (eg.: Nazareth y Hauksson, 2004, Chiarabba y De Gori, 2016, Wu *et al*., 2017 and Zuza y Cao, 2020). The area is divided into a grid of square cells that may or may not overlap. The depth distribution of earthquakes inside each cell is then calculated and assigned to the whole cell. Cells with low earthquake density (usually less than 10 events per cell) are discarded as they are not statistically significant. Here we tested different parameters (see supplementary material) and found the best results with cells of 1.2º width, with a 75% overlap with adjacent cells, resulting in a final cell size of 0.2°. Cells with less than 10 earthquakes were discarded. Figure 2 shows said grid.

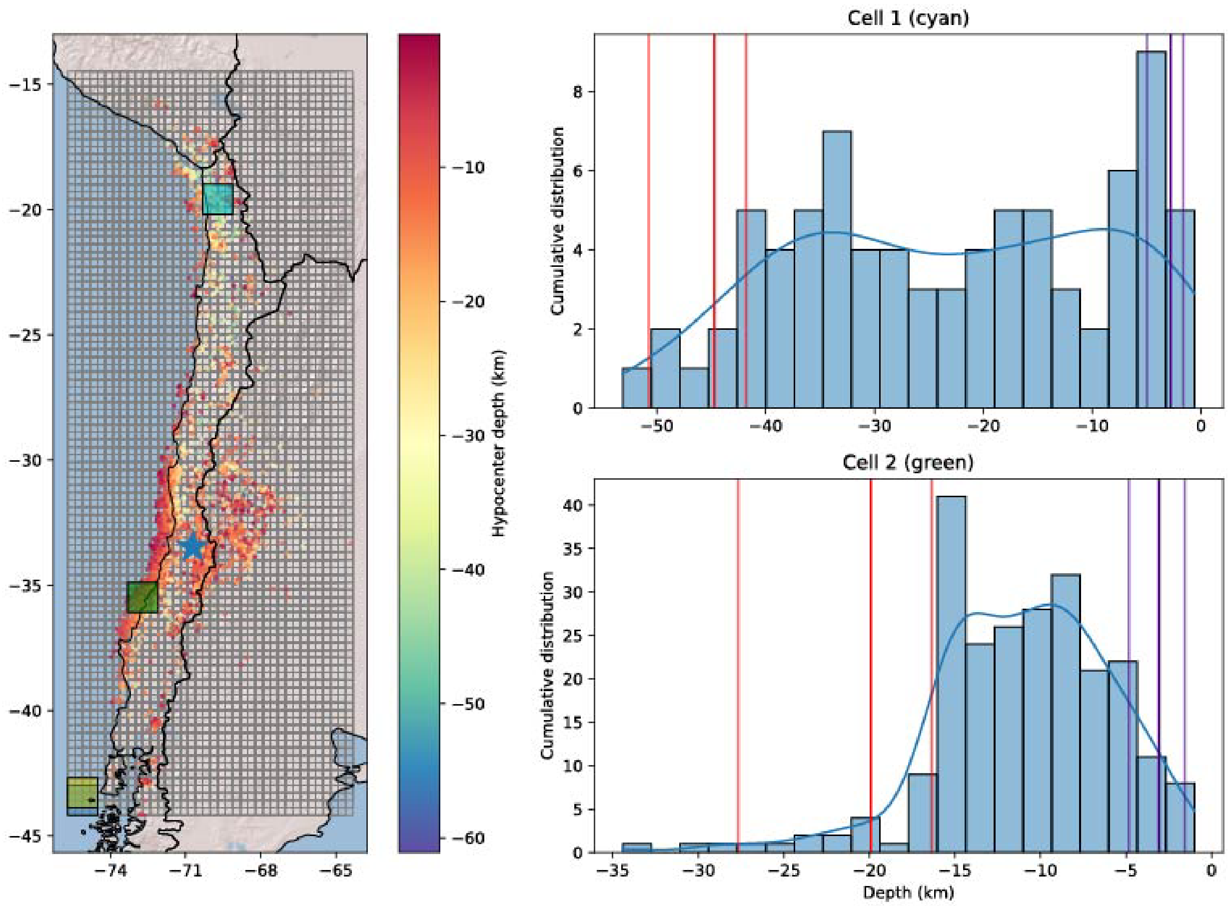

Figure 2: Map (left) of the grid obtained when using the square grid method. On the lower left corner to colored cells, one blue and one yellow are used to show cell size and overlap. Two other cells are colored (cyan and green) and the depth distribution of events on them is graphed (right) Purple lines show D1-10 and red show D90-99.

While the square grid methodology has been widely used, we find it has flaws. In regions where crustal seismicity is heterogenous it results in some cells having a significantly lower statistical significance (ie. less earthquakes) than other cells. Furthermore, it could be better to vary mapping resolution with earthquake density, with a high-resolution mapping for areas with high earthquake density. This method does not allow such flexibility. Therefore, we also employ a new approach where we create a grid of nodes from which a circular cell grows until it encompasses a set number of earthquakes. In this way, all cells have the same statistical significance, and the resulting calculation has higher resolution on regions where hypocenter locations are denser. Like with the square grid method, we tested different parameters on the circular grid and obtained the best results with a grid with 0.4º spacing between nodes and cells that grow until they contain 10 earthquakes to a maximum radius of 0.6º and a minimum radius of 0.3º. Should more than 10 earthquakes be found within less than 0.3º of the node, the cell grows to the set minimum radius instead (here 0.3º) to account for areas with extremely high event density.

3 Results

3.1. SOD and SCD determination

For SOD D1, D5 and D10 were calculated, obtaining similar results with the square (figure 3) and circular (supplementary material) methods. However, the circular grid method results in a slightly more detailed map. All three layers have practically the same geometry with the main obvious difference that D1 is shallower than D10. There is on average a 2.6 km difference between these two layers. Therefore, and to keep our analysis concise, we will focus on D5. This is mostly shallower than 5 km, particularly along the trench and the volcanic arc. Some deeper spots can be found along the Central Valley, between the two previous geologic settings where continental crust is cold and rigid. These deeper areas reach around 8 km with a few localized spots reaching 15-20 km, located on northern Chile (north of 26ºS).

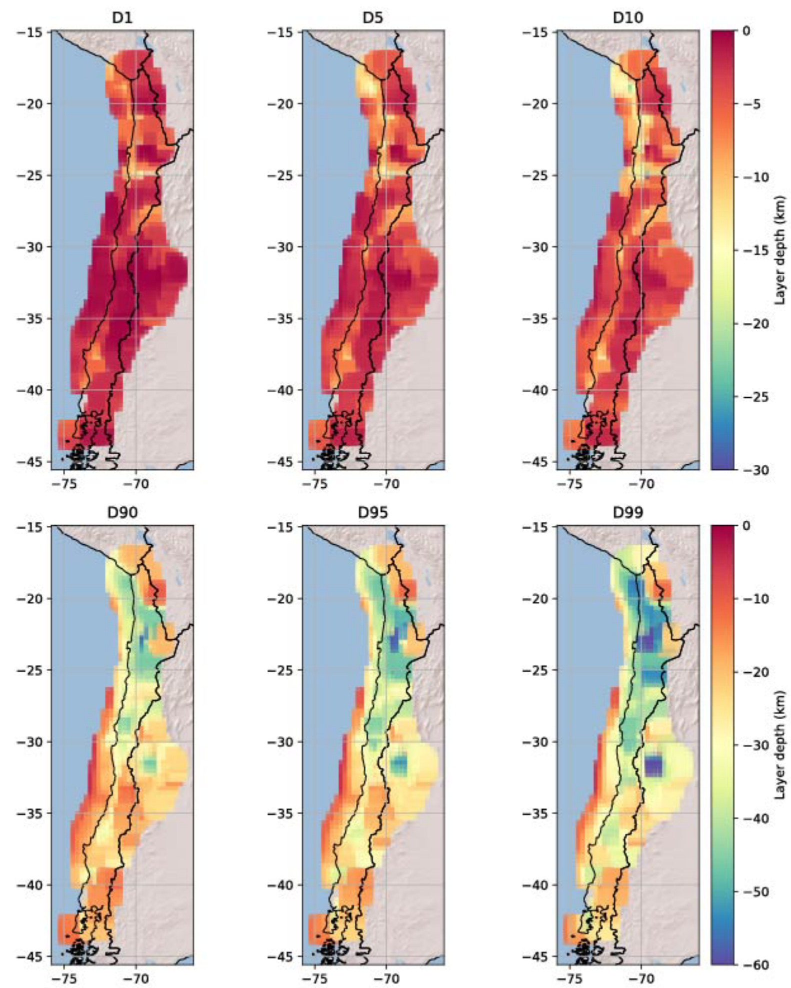

Figure 3: Maps of SOD (D1, D5 and D10) and SCD (D90, D95 and D99) as obtained with the square grid method. The color scale on each map shows the depth of each layer.

For SCD we calculated D90, D95 and D99, and obtain similar results with the square (figure 3) and circular (supplementary material) methods, with more detail obtained with the circular method. These layers have a minimum depth of ~5 km and a maximum of ~60 km. Shallow areas are naturally larger on D90 than D99 and, likewise, deep areas (~60 km) are larger and more abundant on D99. There is on average a 7.7 km difference between the two.

We will focus our analysis on D95 as the estimator of SCD. This layer shows a general tendency of being deeper on northern Chile and shallower towards the south. However, the main changes in its geometry occur in a longitudinal direction. Here, three segments with different behavior can be recognized. North of 25ºS D95 is shallow along the trench (~15-20 km) deepens towards the Central Valley, reaching as deep as 60 km (almost the entire thickness of the continental crust on an area where anomalously deep seismicity has been recorded) and becomes shallow again along the Central Volcanic Zone of the main Andes (~10-15 km). Between ~25ºS and ~33ºS D95 is shallow at the trench (~10-15 km) and becomes deeper towards the Central Valley, reaching depths between 30 and 40 km. Unlike before, it does not become shallower towards the main Andean range and its depth remains constant. In this segment, a particularly deep spot is located undeneath the main Cordillera reaching around 50 km depth. This thick seismogenic segment correlates with a gap of the volcanic arc. South of ~33ºS the same behavior as in the northern segment takes place. D95 is shallow along the margin (~10 km), deep below the Central Valley (~30 km) and shallow again at the active Southern Volcanic Zone of the Andes (~15-20 km).

3.2. Seismic Thickness

Since no clear percentile is used in literature to determine Ts, we follow Wu *et al.* (2017) and use the difference between D99-1, D95-5 and D90-10 to obtain maximum, intermediate and minimum estimations respectively (supplementary material). Here, we only discuss the results obtained for D95-D5, calculated using the square and circular grid methods (figure 4A). Both result in the similar geometry and thickness with small, local differences owing to the better details of the circular grid. The data was then interpolated using linear interpolation to generate a continuous 3D surface (figure 4B).

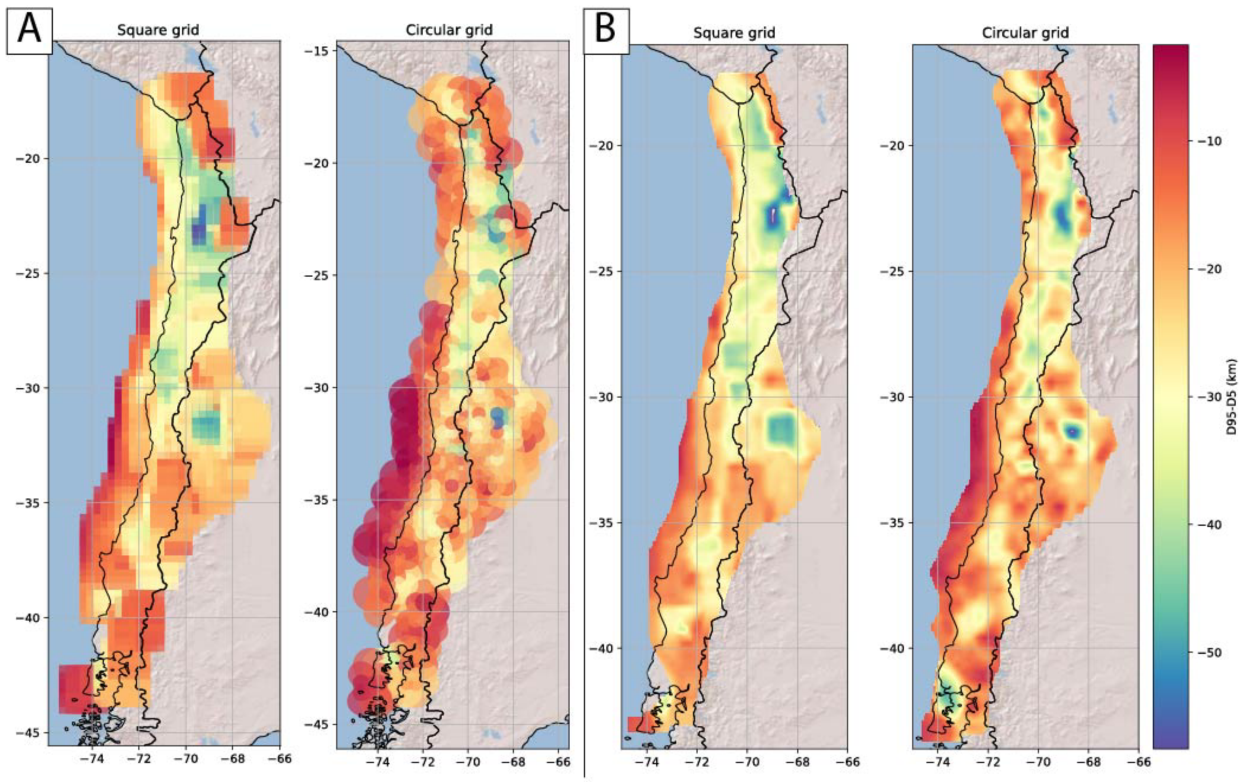

Figure 4: A) Maps of D95-D5 obtained with the square (left) and circular (right) methods. B) Interpolated surfaces obtained from the square (left) and circular (right) methods. The color scale shows layer thickness.

As shown by figure 4, Ts has a similar behavior to D5 and D95. It is generally thicker in northern (~40-50 km below the Central Valley) versus southern (20-30 km below the Central Valley) Chile. Also, like D95, it is latitudinally segmented. North of ~25ºS and south of ~33ºS it is thin at the trench and forearc, becomes thicker below the Central Valley and thinner again in the Cordillera. This trend is interrupted between 25º and 33ºS, where no thinning of Ts is observed associated to the volcanic gap (figure 4). Lastly, there is a local anomaly of high Ts thickness at 31ºS, 69ºW, where D5 is particularly shallow and D95 is anomalously deep.

3.3. Location error

The CSN seismic catalogue, contains an average horizontal error of 5.2 km and average vertical error of 10.2 km. When filtering the catalogue, we discarded all events with either horizontal or vertical error over 15 km. We then calculated the average error within each cell of our grid in the square and circular grid methods (supplementary material).

Average location errors within each cell range between 2 and 6 km. Most cells have an error of ~4 km. There appears to be no correlation between location error and Ts (i.e., thick or thin Ts is independent of cells with high or low location error). Only one exception can be found on the anomalously thick Ts spot at 31ºS, 69ºW which also contains a high location error (~6 km).

4 Discussion

4.1. SOD, SCD and Ts

Our result show that SOD, SCD and Ts vary with two general trends along the Chilean margin. Firstly, SCD is deeper and Ts thicker on northern Chile, where the continental crust is thickest (70-65 km; Tassara and Echaurren, 2012). To the south, the crust becomes progressively thinner, down to ~30 km. Likewise, SCD becomes shallower and Ts thinner. Therefore, it seems Ts thickness is directly related to crustal thickness, likely owing to differences in the thermal gradient which would be the main controlling factor.

Secondly Ts is thin close to the trench and on the volcanic arc, while it is thick bellow the Central Valley which results in 3 longitudinal strips of thin-thick-thin Ts. This geometry is likely controlled by two factors. On and close to the trench, subduction geometry plays a major role, locally controlling Ts. As the slab deepens and continental crust thickens away from the trench, so does Ts. This thickening toward the east and away from the trench does not continue infinitely and Ts start to thin near the volcanic arc, requiring a different control.

Chiarabba y De Gori (2016), Wu *et al*. (2017) and Zuza y Cao (2020), among others, have observed a relationship between SCD, Ts and the BDT. This establishes a direct relationship between Ts and thermal structure: when the crust is hot, BDT is shallow and Ts is thin. In the Chilean case, the volcanic arc has abundant magmatism and thus hot crust, explaining the thin Ts in this area. There is however one central segment between ~25º and 33ºS where Ts does not become thin at Cordillera. This segment coincides almost perfectly with the flat slab which occurs between ~27ºS and 33.5ºS (Ramos y Folguera, 2009). Here there is no mantle wedge between the upper plate and the slab, inhibiting the magmagenesis and therefore the crust has a lower temperature. This accounts for the lack of a thin Ts at the arc between these latitudes.

Within the central segment, there is a local high thickness anomaly in Ts at 31ºS, 69ºW. This anomaly coincides with a higher average location error for cells at those coordinates. However, even if SCD was considered to be 6 km thinner on that spot (average location error for those cells) Ts would still be thicker there than in the surroundings. This high seismogenic thickness may be related to flat slab geometry and/or local lithology. It coincides with the center of the Cuyania terrane accreted to the South American margin at ~460 Ma (Ramos, 2004). This terrane has been shown to have a mafic composition, cold temperature and high seismic velocity (Ramos, 2004, Marot *et al.,* 2014 and McGroder *et al.,* 2015). Furthermore, it is located in an area where the intracrustal disconuity of Tassara and Echaurren (2012) is particularly shallow (0-5 km) and the Moho deep (over 60 km). The combination of these factors, mainly low temperature and mafic crustal composition are likely responsible for the thick Ts in the area.

4.2 Considerations for seismic hazard assessment.

Chile is a seismic country where large subduction earthquakes are abundant. This has resulted in strong building regulations to create earthquake resistant structures, which focus mainly on interplate events and considers 3 hazard zones, parallel to the trench. Thus, the zone closest to the trench is considered to have a high hazard while the one furthest away, and close to the volcanic arc is considered to have a low seismic hazard. While this makes sense considering subduction earthquakes reach the highest magnitudes, crustal earthquakes should not be disregarded.

As previously stated, areas with thin Ts tend to concentrate most crustal earthquakes. However, their rupture depth and therefore magnitude is limited. On the contrary, fewer earthquakes occur on areas with thick Ts, yet they're ruptures could theoretically be thicker, allowing higher magnitudes.

In Chile's case we observe that few earthquakes occur where Ts is thick. A review of the largest crustal events registered in the country (eg. 1958 Ms 6.9 Las Melosas, 2001 Mw 6.3 Chusmiza, 2004 Mw 6.4 Curico and 2010 Mw 6.9 Pichilemu earthquakes) demonstrates that all of them have hypocenters on areas with thin Ts. Furthermore, paleoseismic studies have shown the occurrence of at least two Mw~7.4 events on the San Ramon Fault (Vargas *et al.,* 2014). Such magnitude would require the rupture of the entire fault length (~50 km) with a ~15 km thickness which coincides with our calculated Ts for that area (east of Santiago). Therefore, while thin Ts limits earthquake magnitudes, a ~15 km thickness is still enough to produce large, potentially destructive events. On the remote chance that a crustal earthquake was to rupture the entire seismogenic crust on an area with thick Ts, it would have the potential to reach higher magnitudes. However, considering the historical seismic record, we believe this to be unlikely as crustal stresses are probably insufficient for such an event.

Considering this information, we believe that our results could be used to: 1) Improve the Chilean building norm, to include seismic hazard from crustal earthquakes and 2) Focus research of crustal faults on areas of thin Ts, possibly aiding the discovery of previously unmapped faults.

4.3. Method comparison

We calculated SOD, SCD and Ts with the traditional square grid method and our new circular grid method. Overall, the depth and geometry obtained for all layers is similar on both approaches (Figure 4), but locally, especially on areas with small changes or local anomalies in Ts the circular method obtains more detailed results. This demonstrates the robustness of our results. Furthermore, it validates the circular grid method which we believe it is conceptually better than the square grid method.

The traditional square grid method holds two main flaws. Firstly, all cells have different statistical relevance. Secondly, cell size has to be set according to the areas with least earthquake density, otherwise spatial coverage would be lost. Both of these flaws are increased on areas with heterogenous seismicity, like the Chilean case.

The circular grid method proposed here solves this problem by making cell size dependent on earthquake density rather than be fixed. A set number of events per cell can be chosen making all of them have the same statistical significance. Cells will grow from a central node up to a radius that contains the set number of events, making map resolution a flexible parameter. In the square grid method cells with less than a set number of earthquakes (usually 10) are discarded for not being considered statistically significant. Here, cells that grow beyond the set maximum radius (i.e., they have too few earthquakes over too large an area) are discarded. This also has the advantage of directly displaying earthquake density through cell size while the square grid method would require a separate figure.

5 Conclusions

We calculated Ts on the Chilean margin using data from the CSN network on a traditional square grid and a new circular grid method obtaining better resolution with the circular grid. Our results show there are two tendencies on Ts thickness and geometry. Latitudinally, Ts becomes thinner from north to south. Longitudinally, it is thin near the trench, becomes thicker towards the east, to reach a maximum below the Central Valley and then starts to thin out further east, towards the arc. There is an exception to this behavior approximately between 25ºS and 33ºS where no thinning of Ts occurs at the orogen. This segment coincides with flat slab subduction and a volcanic gap.

These results demonstrate that Ts is mainly controled by the thermal structure of the crust. We anticipate an inverse correlation between Ts and crust temperature, which coincides with the results obtained by Chiabarra y De Gori (2016) and Zuza y Cao (2020). As they impact temperature distribution, crust thickness and subduction geometry may also hold a secondary, indirect, influence. Further work regarding thermomechanical modeling may be done to better constrain BDT and its relationship to Ts in Chile. Lastly, a lithological control on Ts could also be inferred but our current data is insufficient to prove this point.

These results have implications for seismic hazard assessment. Areas with thin Ts should be considered as prone to crustal seismicity. On our maps these areas are located along the coast and the volcanic arc. They coincide with the location of most mapped crustal faults and are also close to many cities.

Acknowledgments

This research was founded by ANID (Agencia Nacional de Investigacion y Desarrollo) through the National Doctorate Grant to MR (Beca de Doctorado Nacional) and Project NCN19_167 Millenium Nucleus CYCLO (The Seismic Cycle along Subduction Zones). We also thank the CSN for providing the necessary seismic data.

Open Research

The data used here to calculate Ts consists of the Centro Sismológico Nacional’s (CSN) seismic catalogue and is freely distributed by the CSN at https://evtdb.csn.uchile.cl/. The code to perform the calculations was developed by the authors and is available at https://doi.org/10.7910/DVN/SBYJKL.

References

Ammirati, J.-B., Vargas, G., Rebolledo, S., Abrahami, R., Potin, B., Leyton, F., & Ruiz, S. (2019). The Crustal Seismicity of the Western Andean Thrust (Central Chile, 33°–34° S): Implications for Regional Tectonics and Seismic Hazard in the Santiago Area. *Bulletin of the Seismological Society of America*, *109*(5), 1985–1999. https://doi.org/10.1785/0120190082

Armijo, R., Rauld, R., Thiele, R., Vargas, G., Campos, J., Lacassin, R., Edgar Kausel, & Kausel, E. E. (2010). The West Andean Thrust, the San Ramón Fault, and the seismic hazard for Santiago, Chile. *Tectonics*, *29*(2). https://doi.org/10.1029/2008tc002427

Burov, E., & Watts, A. B. (2010). *The Equivalent Elastic Thickness (Te), seismicity and the long-term rheology of continental lithosphere. 2010*. https://doi.org/10.1016/j.tecto.2009.06.013

Cahill, T., & Isacks, B. L. (1992). Seismicity and shape of the subducted Nazca plate. *Journal of Geophysical Research: Solid Earth*, *97*(B12), 17503-17529. https://doi.org/10.1029/92JB00493

Campos, J., Ruiz, S., Ruiz, J., Kausel, E., Thiele, R., Saragoni, R., & Sepúlveda, S. (2005). Terremotos corticales de las Melosas 1958, Chusmiza 2001 y Curicó 2004: un análisis comparativo con los terremotos de Northridge 1994 y Kobe 1995: Nuevos antecedentes para el peligro geológico.

Chiarabba, C., Claudio Chiarabba, De Gori, P., & De Gori, P. (2016). The seismogenic thickness in Italy: Constraints on potential magnitude and seismic hazard. *Terra Nova*, *28*(6), 402–408. https://doi.org/10.1111/ter.12233

Eaton, J. P., Lee, W. H. K., & Pakiser, L. C. (1970). Use of microearthquakes in the study of the mechanics of earthquake generation along the San Andreas fault in central California. *Tectonophysics*, *9*(2-3), 259-282. https://doi.org/10.1016/0040-1951(70)90021-1

Hayes, G. P., Ginevra L. Moore, Moore, G. L., Moore, G., Portner, D. E., Hearne, M., Flamme, H., Furtney, M., & Smoczyk, G. M. (2018). Slab2, a comprehensive subduction zone geometry model. *Science*, *362*(6410), 58–61. https://doi.org/10.1126/science.aat4723

Kendrick, E., Bevis, M., Smalley, R., Brooks, B. A., Vargas, R. B., Lauría, E., Luiz Paulo Souto Fortes, & Fortes, L. P. S. (2003). The Nazca -South America Euler vector and its rate of change. *Journal of South American Earth Sciences*, *16*(2), 125–131. https://doi.org/10.1016/s0895-9811(03)00028-2

Maldonado, V., Contreras, M., & Melnick, D. (2021). A comprehensive database of active and potentially-active continental faults in Chile at 1:25,000 scale. *Scientific Data*, *8*(1), 20–20. https://doi.org/10.1038/s41597-021-00802-4

Marcelo Farías, de Farias, M. S., Farías, M., Comte, D., Roecker, S. W., Carrizo, D., & Pardo, M. (2011). Crustal extensional faulting triggered by the 2010 Chilean earthquake: The Pichilemu Seismic Sequence. *Tectonics*, *30*(6). https://doi.org/10.1029/2011tc002888

Marot, M., Monfret, T., Gerbault, M., Nolet, G., Ranalli, G., & Pardo, M. (2014). Flat versus normal subduction zones: A comparison based on 3-D regional traveltime tomography and petrological modelling of central Chile and western Argentina (29°–35°S). *Geophysical Journal International*, *199*(3), 1633–1654. https://doi.org/10.1093/gji/ggu355

McGroder, M. F., Lease, R. O., & Pearson, D. M. (2015). Along-strike variation in structural styles and hydrocarbon occurrences, Subandean fold-and-thrust belt and inner foreland, Colombia to Argentina. *Geological Society of America Memoirs*, *212*, 79–113. https://doi.org/10.1130/2015.1212(05)

Mignan, A., & Woessner, J. (2012). *Estimating the magnitude of completeness for earthquake catalogs*. https://doi.org/10.5078/corssa-00180805

Naranjo, J., y Welkner, D. (2004). Informe sobre efectos del sismo del 28 de agosto 2004 en las nacientes del Río Teno, Vll Region. SERNAGEOMIN.

Nazareth, J. J., & Hauksson, E. (2004). The Seismogenic Thickness of the Southern California Crust. *Bulletin of the Seismological Society of America*, *94*(3), 940–960. https://doi.org/10.1785/0120020129

Perez, A., J. A. Ruiz, Ruiz, J., J. A. Ruiz, Ruiz, J. A., Vargas, G., Rauld, R., Rebolledo, S., & Campos, J. (2014). Improving seismotectonics and seismic hazard assessment along the San Ramón Fault at the eastern border of Santiago city, Chile. *Natural Hazards*, *71*(1), 243–274. https://doi.org/10.1007/s11069-013-0908-3

Ramos, V. A. (2004). Cuyania, an Exotic Block to Gondwana: Review of a Historical Success and the Present Problems. *Gondwana Research*, *7*(4), 1009–1026. https://doi.org/10.1016/s1342-937x(05)71081-9

Ramos, V. A., & Folguera, A. (2009). Andean flat-slab subduction through time. *Geological Society, London, Special Publications*, *327*(1), 31–54. https://doi.org/10.1144/sp327.3

Sibson, R. H. (1982). Fault zone models, heat flow, and the depth distribution of earthquakes in the continental crust of the United States. *Bulletin of the Seismological Society of America*, *72*(1), 151–163.

Riedel, Martin, 2023, "Seismogenic Thickness calculation", https://doi.org/10.7910/DVN/SBYJKL, Harvard Dataverse.

Sielfeld, G., Lange, D., & Cembrano, J. (2019). Intra-Arc Crustal Seismicity: Seismotectonic Implications for the Southern Andes Volcanic Zone, Chile. *Tectonics*, *38*(2), 552–578. https://doi.org/10.1029/2018tc004985

Sippl, C., Schurr, B., G. Asch, Asch, G., Asch, G., & Kummerow, J. (2018). Seismicity Structure of the Northern Chile Forearc From >100,000 Double-Difference Relocated Hypocenters. *Journal of Geophysical Research*, *123*(5), 4063–4087. https://doi.org/10.1002/2017jb015384

Tassara, A., & Echaurren, A. (2012). Anatomy of the Andean subduction zone: Three-dimensional density model upgraded and compared against global-scale models. *Geophysical Journal International*, *189*(1), 161–168. https://doi.org/10.1111/j.1365-246x.2012.05397.x

Vargas, G., Klinger, Y., Rockwell, T. K., Forman, S. L., S Rebolledo, S. Rebolledo, Rebolledo, S., Baize, S., Lacassin, R., & Armijo, R. (2014). Probing large intraplate earthquakes at the west flank of the Andes. *Geology*, *42*(12), 1083–1086. https://doi.org/10.1130/g35741.1

Wu, W.-N., Yen, Y.-T., Yin-Tung Yen, Yin-Tung Yen, Hsu, Y.-J., Wu, Y.-M., Lin, J.-Y., & Hsu, S.-K. (2017). Spatial variation of seismogenic depths of crustal earthquakes in the Taiwan region: Implications for seismic hazard assessment. *Tectonophysics*, *708*, 81–95. https://doi.org/10.1016/j.tecto.2017.04.028

Zuza, A. V., & Cao, W. (2020). Seismogenic thickness of California: Implications for thermal structure and seismic hazard. *Tectonophysics*, *782*, 228426. https://doi.org/10.1016/j.tecto.2020.228426